JOURNAL OF SYNCHROTRON RADIATION
ISSN 1600-5775

A novel imaging tool for hepatic portal system using phase contrast technique with hydrogen peroxide-generated O_2 gas

Rongbiao Tang,[a]* Fuhua Yan,[a]* Wei-Min Chai,[a]* Wei Huang,[a] Yanan Fu,[b] Guo-Yuan Yang[c] and Ke-Min Chen[a]*

[a]Department of Radiology, Rui Jin Hospital, Shanghai Jiao Tong University School of Medicine, Shanghai 200025, People's Republic of China, [b]Shanghai Institute of Applied Physics, Chinese Academy of Sciences, Shanghai 201204, People's Republic of China, and [c]Neuroscience and Neuroengineering Center, Med-X Research Institute, Shanghai Jiao Tong University, Shanghai 200030, People's Republic of China. *Correspondence e-mail: tangme8688258@sina.com, yfh11655@rjh.com.cn, chai_weimin@126.com, keminchenrj@163.com

Received 27 January 2015
Accepted 25 May 2015

Edited by A. Momose, Tohoku University, Japan

Keywords: X-ray phase contrast imaging; O_2 gas; hepatic portal vein; hydrogen peroxide.

Supporting information: this article has supporting information at journals.iucr.org/s

The objective of this study was to investigate the potential of hydrogen peroxide-generated oxygen gas-based phase contrast imaging (PCI) for visualizing mouse hepatic portal veins. The O_2 gas was made from the reaction between H_2O_2 and catalase. The gas production was imaged by PCI in real time. The H_2O_2 was injected into the enteric cavity of the lower sigmoid colon to produce O_2 in the submucosal venous plexus. The generated O_2 gas could be finally drained into hepatic portal veins. Absorption contrast imaging (ACI) and PCI of O_2-filled portal veins were performed and compared. PCI offers high resolution and real-time visualization of the O_2 gas production. Compared with O_2-based ACI, O_2-based PCI significantly enhanced the revealing of the portal vein *in vivo*. It is concluded that O_2-based PCI is a novel and promising imaging modality for future studies of portal venous disorders in mice models.

1. Introduction

Portal vein imaging is an important modality to investigative portal venous diseases, such as portal vein thrombosis, arteriovenous malformation and portal hypertension (Sangster *et al.*, 2013; González *et al.*, 2009; Lee *et al.*, 2008). In the clinic, CT angiography is commonly used for showing portal veins. Digital subtraction angiography is considered as a gold standard for the diagnosis of the disorders. However, these conventional absorption contrast imaging (ACI) techniques need to employ iodine as the contrast agent. Iodine dye may induce nephrotoxicity. Accidents may occur if a patient has an allergic reaction to iodine. In addition, fine vessels can hardly be detected by conventional X-ray imaging methods due to the limitation of spatial resolution.

Synchrotron radiation phase contrast imaging (PCI) has been claimed to have the potential for biomedical applications (Bravin *et al.*, 2013; Lewis, 2004). Blood vessels down to the micrometre level can be markedly revealed by PCI using air as the contrast agent (Zhang *et al.*, 2008; Laperle *et al.*, 2008). PCI can also offer more detailed images for soft tissues by analyzing the phase shift effect of the beam (Tang *et al.*, 2013*a*, 2012*a*,*b*; Wilkins *et al.*, 1996; Momose *et al.*, 1996). Owing to the different refractive index between gas and soft tissues, the phase shifts caused by the gas–tissue interfaces can make the boundaries highly visible in PCI (Tang *et al.*, 2013*b*, 2011; Xi *et al.*, 2011; Davis *et al.*, 1995). By detecting the phase shift produced between the vascular wall and O_2, PCI may facilitate clearer visualization of O_2-filled portal veins.

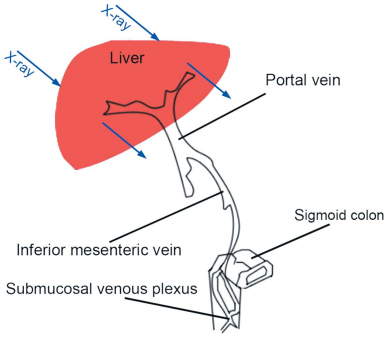

It is known that mouse blood has catalases that can catalyze the decomposition of hydrogen peroxide to form water and oxygen gas. The equation of the chemical reaction is $2H_2O_2 \rightarrow 2H_2O + O_2$. Without catalysis, this reaction occurs spontaneously but very slowly. H_2O_2 can be intestinally absorbed into the submucosal venous plexus after it is injected into the intestine. Then H_2O_2 reacts with catalases in the blood of the venous plexus to produce O_2 gas. Finally, the generated O_2 gas is drained into the inferior mesenteric veins and then to the portal veins.

Thus, the purpose of our study was to prospectively evaluate the use of H_2O_2-generated O_2 as a PCI contrast agent for imaging the hepatic portal vein in living mice.

2. Methods

2.1. Main synchrotron radiation parameters

Imaging was performed at the BL13W1 beamline in the Shanghai Synchrotron Radiation Facility (SSRF). The energy range of the beamline was 8–72.5 keV. The photon density at the sample position was 5×10^{10} photons s^{-1} mm^{-2} at 20 keV. The X-rays originated from a 3.5 GeV electron storage ring and were monochromated using a double-crystal monochromator combined by a Si(111) orientation crystal and a Si(311) orientation crystal. The transmitted X-rays were first converted to visible light by a scintillator consisting of a 100 µm-thick $CdWO_4$-cleaved single-crystal, and then transformed into an image by a CCD camera. Samples were placed on an M-840 HexaLight six-axis stage (Physik Instrumente, Germany) at a distance of 34 m from the synchrotron source. The distance between the sample and the detector could be varied up to 8 m. A diagram of the setup is presented in Fig. 1.

2.2. PCI of O_2 gas production

A 3% hydrogen peroxide solution was placed in a polyethylene tube, which was perpendicular to the X-ray beam (Fig. 2*a*). Fresh mouse blood was injected into the H_2O_2 solution through a PE-50 tube connected to a computer-controlled syringe pump. In accordance with the previous research in our experimental hutch (Tang *et al.*, 2011; Xiao *et al.*, 2005), in-line PCI was performed at an energy of 19 keV with a sample-to-detector distance of 60 cm. Images were consecutively captured using an X-ray Image VHR 1:1 detector (Photonic Science, UK) with a 9 µm pixel size. The spatial resolution and the designed time resolution of images taken by this detector were about 18 µm and 1.0 ms per frame, respectively.

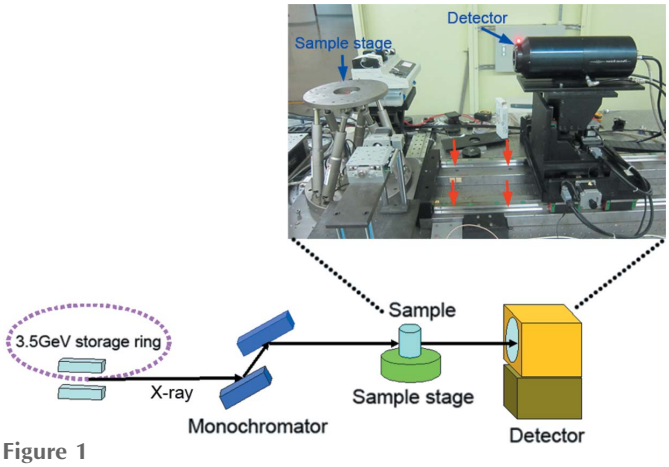

Figure 1
Schematic of the experimental setup for in-line PCI at BL13W in SSRF. The distance between the radiation source and the sample stage was 34 m. The energy of the monochromatic X-rays was chosen at 19 keV. The inset shows the detector on the rail (red arrows) which can move between 0 and 8 m from the sample stage.

2.3. Animals

All animal surgical procedures and experimental protocols were reviewed and approved by the Institutional Animal Care and Use Committee and the Ethics Committee of Shanghai Jiao Tong University. ICR mice were bought from the Animal

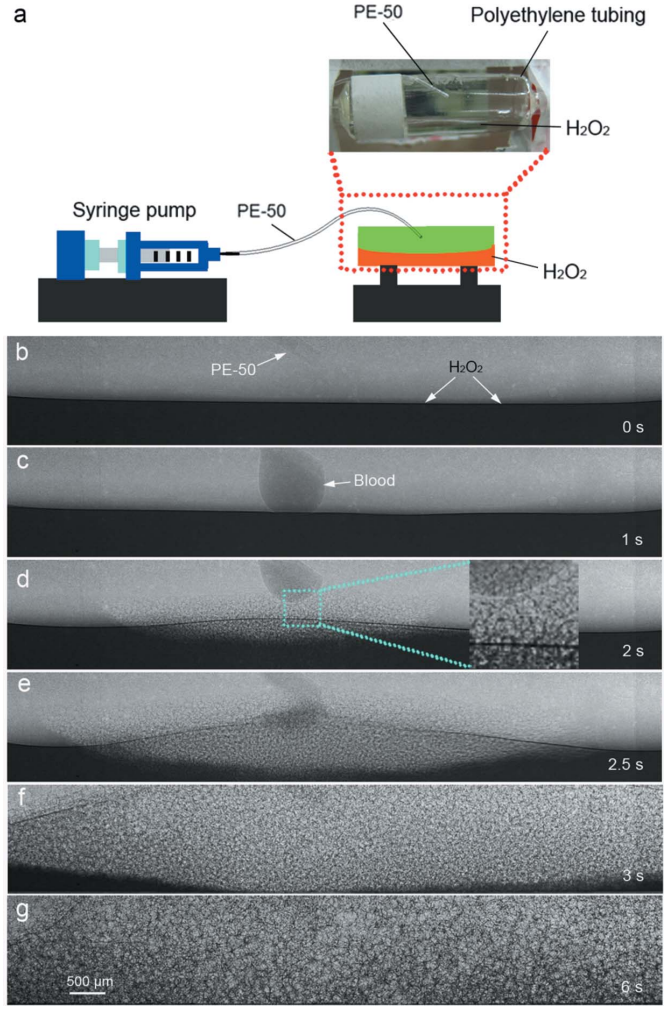

Figure 2
Representative sequential PCI of O_2 gas production. (*a*) The experimental setup for generating O_2 gas. O_2 gas bubbles were clearly shown to be continuously produced after H_2O_2 encountered catalases in the mouse blood. Images were attained following the blood injection at 0 s (*b*), 1 s (*c*), 2 s (*d*), 2.5 s (*e*), 3 s (*f*), and 6 s (*g*), respectively. The pixel size was 9 µm × 9 µm; the exposure time was 8 ms.

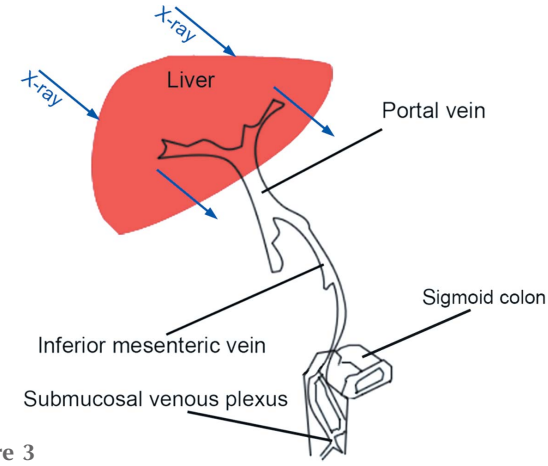

Figure 3
Schematic for the portal tract from the submucosal venous plexus to the main portal vein. H_2O_2 reacted with catalase to give out O_2 gas after it was intestinally absorbed into the submucosal venous plexus of the lower sigmoid colon. The generated O_2 bubbles were drained into the inferior mesenteric vein and then to the portal vein. The liver was placed perpendicular to the monochromatic X-rays.

Center, CAS, Shanghai, China. Animals were housed in a temperature-controlled room with a 12 h light–dark cycle and acclimatized for at least seven days before use. Prior to imaging, food was withheld for 24 h with free access to water.

2.4. O_2-based PCI for visualizing the portal vein in living mice

A mid-line abdominal incision was made for ICR mice after anesthesia. A part of the hepatic lobes was bent and protruded from the abdomen in order to obtain a projection image of the liver. Then, 0.3 ml of 3% H_2O_2 was injected into the enteric cavity of the lower sigmoid colon using a 1 ml syringe (BD). A schematic is given in Fig. 3. ACI and PCI were performed with sample-to-detector distances of 1 cm and 60 cm, respectively. Images were obtained using a PCO 2000 camera (Optique Peter optical system) with a 3.7 µm pixel size. Relative densities were assessed by line profile analysis *via Image-Pro Plus 6.0*.

3. Results

3.1. Real-time PCI of O_2 gas production

No O_2 gas bubbles could be found before blood injection (Fig. 2*b*). After adding the blood, O_2 bubbles were clearly shown to be continuously generated (Figs. 2*c*–2*g*). PCI could also present the real-time visualization of the reaction process (supplementary movie 1).

3.2. ACI and PCI of the hepatic portal vein *in vivo*

Before the H_2O_2 injection, blood-filled vessels could not be imaged at all in PCI (Figs. 4*a* and 4*b*). Because the difference between the absorption coefficients of the vascular wall and the O_2 gas was small, poor contrast could be detected by ACI (Figs. 4*d* and 4*e*). In comparison, PCI exploited the differences in the refractive index and enabled clear revelation of the portal vein system (Figs. 4*g* and 4*h*). A more visible change in intensity around the vascular edge was detected by PCI (Fig. 4*i*). The smallest diameter of the O_2 gas-filled portal veins was about 25 µm. O_2 gas was found to gradually dissolve in the portal veins over time *in vivo* (Fig. 5).

4. Discussion

Air has been shown as an ideal candidate for phase contrast X-ray angiography (Lundström *et al.*, 2014; Tang *et al.*, 2011; Laperle *et al.*, 2008). After excised livers are fixed and dehydrated, all liver vessels will be filled with air to replace the blood, so that the air-filled vessels can be definitely detected by PCI (Laperle *et al.*, 2008). However, using this method, we can hardly distinguish between portal veins, hepatic arteries and hepatic veins in the excised livers. Carbon dioxide gas and physiological saline have been considered to be quite suitable PCI contrast agents (Takeda *et al.*, 2012, 2002; Lundström *et al.*, 2012*a*,*b*; Zhang *et al.*, 2008). The contrast agents have

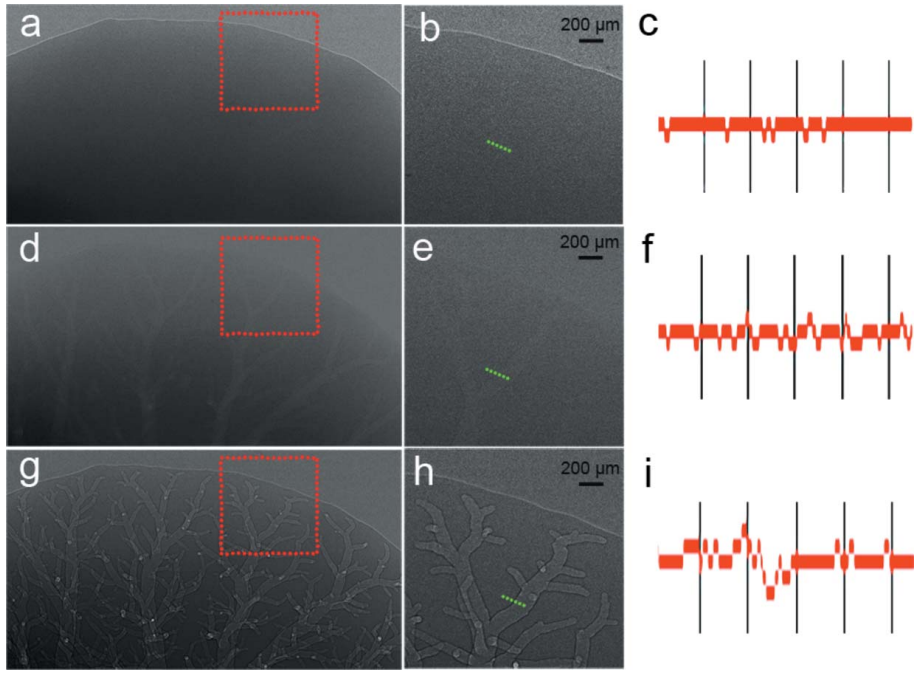

Figure 4
In vivo synchrotron radiation images of mouse portal veins before and after H_2O_2 injection: (*b*), (*e*) and (*h*) are magnified images of the red boxed regions in (*a*), (*d*) and (*g*), respectively. Note that no vessels are displayed before H_2O_2 injection (*b*), and the portal vein could be more visibly revealed with PCI (*h*) than with ACI (*e*). Views (*c*), (*f*) and (*i*) are the line profile analyses of intensity values along a line (green) in (*b*), (*e*) and (*h*), respectively. Note that a distinct change in intensity was detected along the vascular wall on the phase contrast image. Images were acquired at 2 min after injection of H_2O_2. ACI and PCI were performed with sample-to-detector distances of 1 cm (*d*) and 60 cm (*a*, *g*), respectively. The pixel size was 3.7 µm × 3.7 µm; the exposure time was 0.5 s.

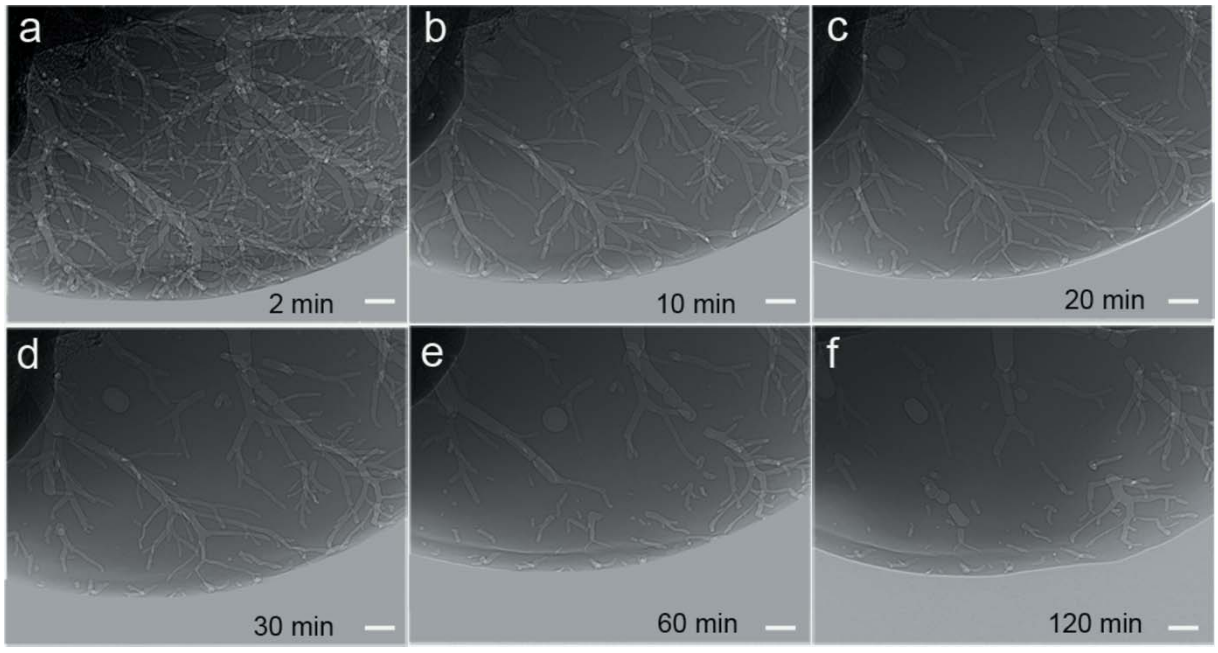

Figure 5
In vivo time course of PCI of mouse portal veins. The minutes post-H_2O_2 injection are denoted in the images. Note that O_2 gas gradually dissolved in the blood of portal veins. Images were obtained with a sample-to-detector distance of 60 cm. The pixel size was 3.7 μm × 3.7 μm; the exposure time was 0.5 s; scale bars: 500 μm.

always been injected into the targeted vessels by surgical catheterization. However, this catheterization process is troublesome and invasive.

In this study, we first used O_2 gas as the in-line PCI contrast agent. Instead of injection, O_2 gas was generated by the reaction between H_2O_2 and the catalase enzyme in the blood, so that the catheterization process could be avoided. Though there is catalase in intestinal epithelial cells that prevents absorption of a low level of H_2O_2, 0.3 ml of 3% H_2O_2 solution is sufficient to produce enough O_2 gas for clearly imaging portal veins in living mice. Additionally, the generated O_2 gas was found to gradually dissolve to recover the blood flow. Therefore, before its clinical application, O_2-based PCI seems to be an attractive imaging modality for investigating disease progression and response to therapy in mice models of portal venous disorders. In the early stages of the diseases, the morphological and architectural changes of the vasculature only occur in fine portal veins. PCI can meet the visualization requirements of these fine vessels by its high discrimination. The subsequent histological examinations for livers will be unaffected because O_2 gas is nontoxic and biocompatible. A limitation to our study was that only two-dimensional projection images, rather than three-dimensional images, were acquired by this imaging modality. In future studies, the use of a detector system with higher temporal resolution may satisfy the needs of rapid image acquisition for three-dimensional visualization.

The characteristic of high spatiotemporal resolution for PCI was rather appropriate for clear and real-time imaging of the reaction process. Compared with ACI, PCI was able to generate outstanding visibility of the O_2-filled portal vein. ACI mainly employs the absorption characteristics of X-rays and distinguishes different tissues through the linear attenuation coefficient, which is proportional to the density of the tissue (Tang *et al.*, 2012*a*, 2011). Little density difference produces poor contrast between gas and the portal vein. In contrast, O_2-based PCI utilizes the phase shifts created by the O_2–vascular wall interfaces and makes edge enhancement more visible.

5. Conclusion

In summary, it is more convenient to use H_2O_2-generated O_2 as a PCI contrast agent than other materials. Oxygen gas-filled portal veins can be clearly visualized by detecting the phase shift with PCI. Although the ICR mice used here do not carry any diseases, it is clear that this novel imaging tool presents a great potential for future studies in mice models of portal venous disorders.

Acknowledgements

This research was supported by the National Natural Science Foundation of China (Grant nos. 81301347 and 81271740), Nation Basic Research Program of China (973 Program 2010CB834305), Shanghai Jiao Tong University Med-Science Cross Research Foundation (YG2013MS30), State Key Clinical Department of Medical Imaging and Shanghai College of first-class discipline.

References

Bravin, A., Coan, P. & Suortti, P. (2013). *Phys. Med. Biol.* **58**, R1–R35.
Davis, T., Gao, D., Gureyev, T., Stevenson, A. & Wilkins, S. (1995). *Nature (London)*, **373**, 595–598.

González, S. B., Busquets, J. C. V., Figueiras, R. G., Martín, C. V., Pose, C. S., de Alegría, A. M. & Mourenza, J. A. C. (2009). *Am. J. Roentgenol.* **193**, 1425–1433.
Laperle, C. M., Hamilton, T. J., Wintermeyer, P., Walker, E. J., Shi, D., Anastasio, M. A., Derdak, Z., Wands, J. R., Diebold, G. & Rose-Petruck, C. (2008). *Phys. Med. Biol.* **53**, 6911–6923.
Lee, H.-K., Park, S. J., Yi, B.-H., Yeon, E.-K., Kim, J. H. & Hong, H.-S. (2008). *Abdom. Imaging*, **33**, 72–79.
Lewis, R. (2004). *Phys. Med. Biol.* **49**, 3573–3583.
Lundström, U., Larsson, D. H., Burvall, A., Scott, L., Westermark, U., Wilhelm, M., Arsenian Henriksson, M. & Hertz, H. M. (2012*a*). *Phys. Med. Biol.* **57**, 7431–7441.
Lundström, U., Larsson, D. H., Burvall, A., Takman, P. A., Scott, L., Brismar, H. & Hertz, H. M. (2012*b*). *Phys. Med. Biol.* **57**, 2603–2617.
Lundström, U., Westermark, U. K., Larsson, D. H., Burvall, A., Arsenian Henriksson, M. & Hertz, H. M. (2014). *Phys. Med. Biol.* **59**, 2801–2811.
Momose, A., Takeda, T., Itai, Y. & Hirano, K. (1996). *Nat. Med.* **2**, 473–475.
Sangster, G. P., Previgliano, C. H., Nader, M., Chwoschtschinsky, E. & Heldmann, M. G. (2013). *HPB Surg.* **2013**, 12.
Takeda, T., Momose, A., Wu, J., Yu, Q., Zeniya, T., Thet-Thet-Lwin, Yoneyama, A. & Itai, Y. (2002). *Circulation*, **105**, 1708–1712.
Takeda, T., Yoneyama, A., Wu, J., Thet-Thet-Lwin, Momose, A. & Hyodo, K. (2012). *J. Synchrotron Rad.* **19**, 252–256.
Tang, R., Chai, W.-M., Yang, G.-Y., Xie, H. & Chen, K.-M. (2012*b*). *PLoS One*, **7**, e45597.
Tang, R., Chai, W.-M., Ying, W., Yang, G.-Y., Xie, H., Liu, H.-Q. & Chen, K.-M. (2012*a*). *Phys. Med. Biol.* **57**, 3051–3063.
Tang, R., Huang, W., Yan, F., Lu, Y., Chai, W.-M., Yang, G.-Y. & Chen, K.-M. (2013*a*). *PLoS One*, **8**, e80919.
Tang, R., Li, W.-X., Huang, W., Yan, F., Chai, W.-M., Yang, G.-Y. & Chen, K.-M. (2013*b*). *Sci. Rep.* **3**, 2312.
Tang, R., Xi, Y., Chai, W.-M., Wang, Y., Guan, Y., Yang, G.-Y., Xie, H. & Chen, K.-M. (2011). *Phys. Med. Biol.* **56**, 3503–3512.
Wilkins, S., Gureyev, T., Gao, D., Pogany, A. & Stevenson, A. (1996). *Nature (London)*, **384**, 335–338.
Xi, Y., Tang, R., Wang, Y. & Zhao, J. (2011). *Appl. Phys. Lett.* **99**, 011101.
Xiao, T., Bergamaschi, A., Dreossi, D., Longo, R., Olivo, A., Pani, S., Rigon, L., Rokvic, T., Venanzi, C. & Castelli, E. (2005). *Nucl. Instrum. Methods Phys. Res. A*, **548**, 155–162.
Zhang, X., Liu, X.-S., Yang, X.-R., Chen, S.-L., Zhu, P.-P. & Yuan, Q.-X. (2008). *Phys. Med. Biol.* **53**, 5735–5743.